Adaptive Assembly Module for Industrial Robot: Design and Simulation

M. Polishchuk
Associate Professor
National Technical University of Ukraine
Department of Technical Cybernetics
Ukraine

S. Telenyk
Professor
National Technical University of Ukraine
Department of Information Systems and Technologies
Ukraine

M. Tkach
Associate Professor
National Technical University of Ukraine
Department of Technical Cybernetics
Ukraine

In modern production, automation of assembly processes is achieved by using industrial robots with high positioning accuracy, as well as with elements of tactile adaptation and expensive software. The article proposes an alternative approach to solving the problem of reducing the cost of assembly processes. This approach consists of using production tooling in the form of a soft adaptive assembly module that is mounted on the robot arm. The proposed assembly module allows not only for compensating for errors in the relative orientation of assembly objects, but also excludes the possibility of damage to fragile assembly components or for assembly objects with a thin protective coating of a chemical or galvanic nature. This effect is achieved due to the use of elastic corrugated chambers in the module structure, which, when compressed air is supplied to them, correct the position of one of the assembly objects.

The article offers a description of the new design of the assembly module, as well as offers analytical dependencies for calculating the design parameters of the module. The results of modeling the parameters of the assembly module are presented. The main economic effect is to reduce the cost of technological equipment for industrial robots while maintaining the ability to adapt to the conditions of the assembly process.

Keywords: *robotic assembly, assembly adaptation, soft gripper, precision connections*

1. INTRODUCTION

In the field of mechanical engineering, the cost of automation of assembly processes dominates due to the need to use equipment with high positioning accuracy of actuators. The most effective tools for automating assembly processes are industrial robots. To compensate for the positioning error, both the robot arm and the peripheral equipment use means of adaptation to the assembly conditions. Such means are tactile or optical sensors for identifying the misalignment error of assembly objects, as well as rather complex software for correcting the position of the robot arm. Taken together, the traditional approach to solving the problem of mismatching assembly objects leads to additional capital investments in the automation of assembly processes. In addition, in the process of prolonged operation of industrial robots, the accuracy of their actuators decreases and these mechanisms require major repairs. This circumstance additionally increases the cost of assembly operations and, as a consequence, the cost of the final product. The special technological equipment of the robot arm, which is designed to compensate for the error in the relative orientation of the assembly objects, allows the use of simple and inexpensive manipulators of industrial robots. These technological devices, as a rule, contain elements of compliance in the form of mechanical springs or vibration drives for stochastic search for the interface of assembly objects. This approach is quite effective for assembling high-strength parts. However, this approach to solving the problem is not acceptable for assembling fragile parts or parts with thin protective chemical or galvanic coatings on their surface.

The article proposes an adaptive assembly module, which is installed on the arm of an industrial robot and allows not only it to compensate for the orientation errors of assembly objects but also excludes the possibility of damage to their surfaces. This effect is achieved as a result of the use of pneumatic corrugated chambers in the module. Due to their deformation, these elastic chambers compensate for errors in the relative orientation of assembly objects without additional dynamic loads. The direction of the initial displacement of the attached assembly object is determined by the difference in pressures of the compressed air in the sections of the elastic chambers. The article also proposes analytical dependencies for the engineering calculation of the parameters of the assembly module and the results of its modeling. The proposed technical solutions allow the robotic assembly of fragile parts or parts with a thin protective coating. Ultimately, the proposed approach makes it possible to increase the efficiency of automation of assembly processes without significant additional capital investments.

2. PREREQUISITES AND MEANS FOR SOLVING THE PROBLEM

The problem of robotization of assembly processes is the need to eliminate the relative mismatch of assembly objects when they are fed to technological positions. This problem is further complicated by the fact that

Received: July 2021, Accepted: November 2021
Correspondence to: M. Polishchuk,
Associate Professor, National Technical University of Ukraine Department of Technical Cybernetics, Ukraine
E-mail: borchiv@ukr.net
doi: 10.5937/fme2201149P

different batches of products differ in permissible deviations in the dimensions of assembly objects [1]. Therefore, initially, it is necessary to improve the accuracy of assembly, as noted in [2]. The most important is to ensure the reliability of the assembly in the conditions of mass production, which uses assembly lines of various types [3]. In modern production, the solution to this problem is carried out in three main directions, namely: 1) identification of the initial position of assembly objects based on optical and tactile sensors with subsequent correction of the position of the attached parts; 2) search for the mating zone of parts based on passive and active adaptation means that are installed on the arm of an industrial robot; 3) the use of anthropomorphic structures of the hand or gripping devices of robots to increase their versatility. Each of these directions for solving the problem of guaranteed assembly is characterized by a different cost and productivity of the assembly process.

The first of these areas of research can be attributed to the use of laser sensors, which are located in the robot's hand and are designed to determine the initial position of assembly objects [4]. Also, vision systems [5] are quite effective for identifying the initial position of the attached component of the assembly or measuring the perpendicularity of parts relative to each other [6]. These methods make it possible to correct the initial position of assembly objects, but for mass production, differentiation of technological operations is inherent to increase productivity. And the installation of these systems at each of the many assembly positions significantly increases their cost.

The means of passive and active adaptation, which are installed on the arm of an industrial robot and belong to the second of the above directions of assembly development, are characterized by a lower cost.

The technical solution [7] can serve as a classic example of passive compliance of the manipulator grip. This assembly device for an industrial robot contains a structure with a distant center of yielding elastic elements that connect the gripper of the manipulator to its body. A dynamic model of the assembly of cylindrical parts taking into account the value of passive compliance is presented in [8]. However, the lack of active influence on assembly parts in these works can lead to the jamming of parts at critical values of the misalignment of assembly objects.

An active stochastic effect on assembly objects is reflected in works [9–12], which use low-frequency vibrations along the trajectories of searching for the mating zone of parts. In these studies, vibrations are communicated to either the attached part or to the base object of the assembly. In [13], an active influence on the assembly component is carried out by combining the rotation of the gripper of an industrial robot and a vibration device. Experimental studies of the improved method using stochastic search for the mating zone of parts are described in [14]. However, the considered means of active adaptation using vibrations are characterized by shock dynamic loads that can lead to damage to fragile parts or parts that have a thin protective coating.

The use of anthropomorphic structures of a hand or gripping devices of robots to increase their versatility belongs to the third of the above directions for improving assembly processes. Anthro–polymorphic grippers for industrial robots are shown in studies [15–18]. In [19], a soft robot arm with tactile feedback is proposed. These technical solutions can be successfully used to grip assembly components, the shape, and position of which are a priori unknown. However, in addition to their high cost, anthropomorphic structures are characterized by low productivity, which is not very suitable for the conditions of mass production.

The above analysis of technical solutions and research in the field of robotization of assembly processes shows that the problem of synthesizing technological equipment for industrial robots in conditions of mass production remains relevant.

3. FORMULATION OF THE PROBLEM

For the successful use of simple and inexpensive industrial robots with low positioning accuracy in mass production conditions, it is necessary to create an adaptive assembly module that is installed on the robot arm to compensate for the relative misalignment of assembly objects. A prerequisite is the ability to assemble fragile products or parts with a thin protective coating of chemical or galvanic origin. In addition, it is necessary to develop analytical dependencies of the parameters of the assembly module, which will enable engineers in this field to design such devices.

4. SOLUTION OF THE PROBLEM UNDER CONSIDERATION

The engineering novelty of the proposed technical solutions lies in a fundamentally new design of an assembly module for an industrial robot (Patent UA No. 120783), and analytical dependences for calculating the parameters and modeling an adaptive assembly module represent scientific novelty. The main motivation for this research is the creation of technological equipment for industrial robots, which allows the assembly of high-precision joints and at the same time eliminates the risk of damage to fragile parts or assembly objects with a thin chemical or galvanic coating of their surface.

4.1 Design of adaptive assembly module

In Figure 1 shows a 3D model of an adaptive assembly module in a quarter section. The assembly module is mounted on the robot arm using a bracket on which a central rod is attached. In the upper part of this rod, there are fixed elastic chambers, namely: an outer corrugated chamber and an inner chamber that is oval. The lower parts of said elastic chambers are connected by a sleeve with an inner tapered hole.

The aforementioned center rod has a taper at its bottom, which forms clearances "*C*" and "*B*" with the tapered bushing. A pneumatic diaphragm actuator is mounted on this sleeve. When compressed air is supplied, said diaphragm moves the piston rod of the pneumatic cylinder. The specified rod through the mechanism of the articulated parallelogram imparts movement to the clamping elements of the gripper to hold the part, which is attached to the assembly.

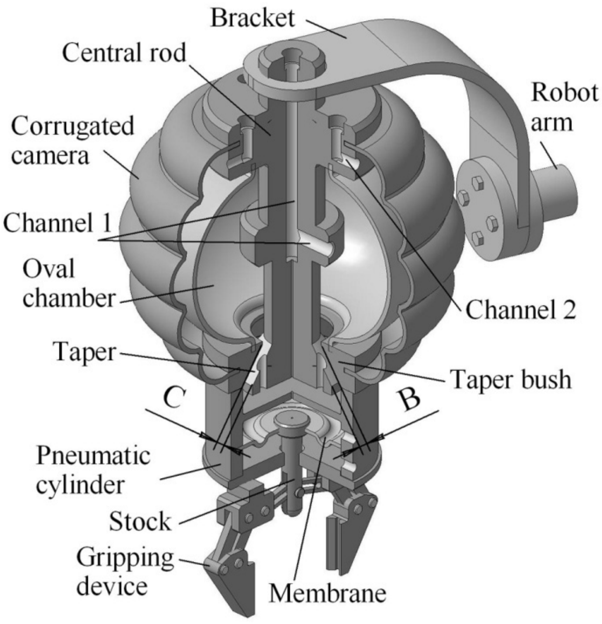

Figure 1. Adaptive assembly module in section ¼ volume

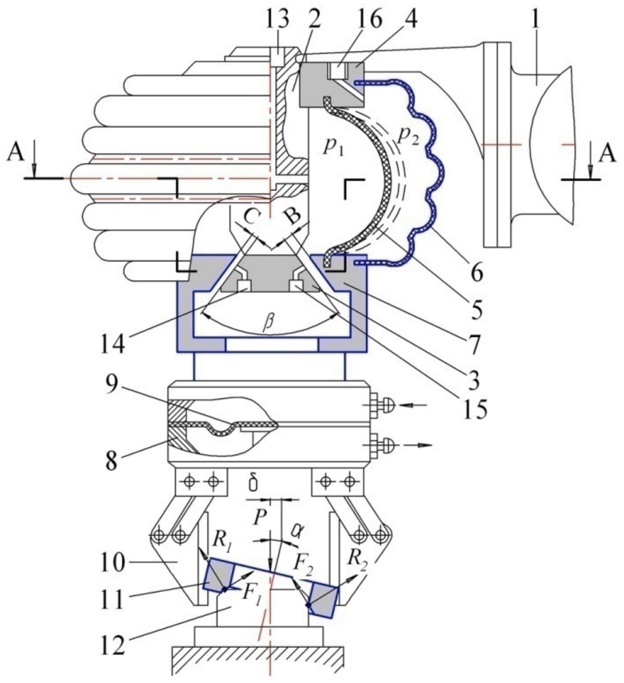

Figure 2. Longitudinal section of the assembly module

Through channel 1, compressed air is supplied to the oval-shaped inner chamber. In the absence of an error in the positioning of the robot arm, the clearances are C = B = 0. But when a linear and angular error occurs in the positioning of the robot arm, under the action of the assembly force, the elastic chamber of the oval shape is deformed, and these gaps $(C \neq D) > 0$ appear with possible combinations $C > D$ or $C < D$ depending on the direction of the positioning error of the robot arm. Then the compressed air that passes through the gaps "C" and "B" creates a pressure difference in them due to the skewed axes of the parts that are assembled into a unit. In proportion to the specified pressure difference in the gaps "C" and "B", compressed air is supplied through channels 2 to different sections of the corrugated chamber to deform it in the direction of compensating for the misalignment of the parts that are being assembled.

Figure 2 shows in more detail a longitudinal section of the assembly module. As noted above, the adaptive assembly module is installed on arm 1 (Figure 2) of an industrial robot using a central rod 2, which has an inverse cone 3 with an angle β at its end.

On rod 2 a ring 4 is installed, in which an oval-shaped elastic chamber 5 is fixed and an elastic corrugated chamber 6. The lower ends of the said elastic chambers 5 and 6 are connected by a ring 7 with a tapered hole. This hole forms annular gaps "C" and "B" with a cone 3. A pneumatic actuator 8 with a diaphragm 9 is installed on ring 7. When compressed air is supplied to the upper or lower cavity of the actuator 8, the diaphragm 9 through the articulated parallelogram transmits the movement to the gripper 10, which holds the part of the type "sleeve" 11 during its assembly with the base part of the type "shaft" 12.

When assembling these parts, due to the linear positioning error "δ" and the angular error "α" under the action of the assembly force P, reaction forces R_1 and R_2, as well as friction forces F_1 and F_2 appear at the points of contact of the parts being assembled. These friction forces, at a certain value, can lead to such a negative phenomenon as jamming of the parts that are being assembled. To avoid jamming of the assembled parts through-hole 13 of rod 2, compressed air is fed into the elastic chamber 5. In this case, the compressed air passes through the annular gaps "C" and "B", which in the case of relative skew of parts 11 and 12 are not equal, for example, C < B or C > B, depending on the direction of the linear positioning error "δ" and the angular error "α" of the assembled parts. When the areas of the annular gaps "C" and "B" are uneven, there are different compressed air pressures in them and holes 14 and 15. The specified pressure difference is monitored by pressure sensors, which are connected to ports 14 and 15. A schematic diagram of the pressure sensor connections is shown in Figure 3. In proportion to this pressure difference, compressed air is supplied through the holes 16 into one of the four sections I, II, III, or IY of the corrugated chamber 6, as shown in Figure 3. Sections of the corrugated chamber 6 are formed by partitions 17. According to the schematic diagram of the control unit, corresponding pressure sensors 18 ... 21 are connected to each of the holes 14 and 15. According to the signals of these sensors, depending on the difference in the compressed air pressure in the gaps "C" and "B", electromagnetic pneumatic valves 22 ... 25 are switched on to supply compressed air to the corresponding sections I, II, III, and IY of the corrugated chamber 6.

The adaptive assembly module operates as follows. For example, if the linear positioning error "δ" and the angular error "α" of the parts that are being assembled correspond to the direction shown in Figure 2, then the gaps "C" and "B" have the ratio C <B. Then, due to the smaller area of the gap "C", the compressed air pressure in it is higher, and in the larger gap "B" the pressure is

lower. The specified pressure difference is measured by the respective sensors 18 and 19 (Figure 3).

Since the smaller cross-section of the annular gap (for example, C<B) coincides with the direction of displacement of part 11, which is attached, then in the particular case shown by way of example in Figure 2, the relay sensor 19 is triggered (Figure 3). As a result, the pneumatic valve 23 is turned on, which supplies compressed air to section IY of chamber 6. This chamber, like other sections, has a corrugated shape along the outer surface. Under the action of pressure, the chamber stretches and moves the gripper 10 with part 11 in the direction of compensating for the positioning error relative to the base part of the type "shaft" 12.

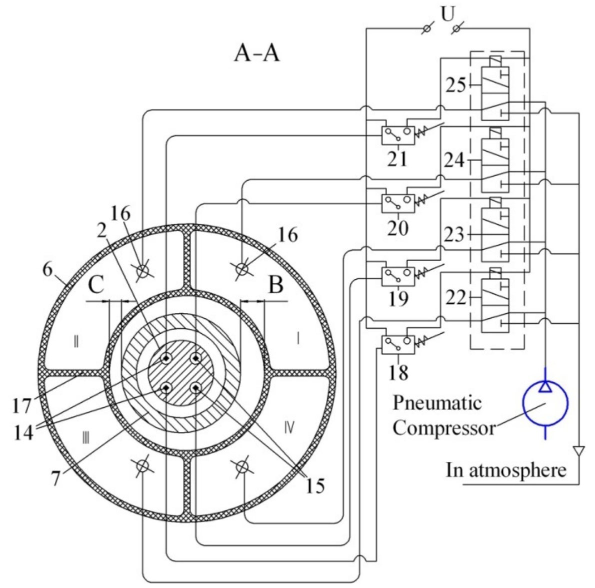

Figure 3. Diagram of connections of pneumatic chambers with pressure sensors (according to section A-A in Figure 2)

The adaptive assembly module, by alternate actuation of sensors 18–21, supplies compressed air through pneumatic valves 22–25 to the corresponding sections I–IV of the corrugated chamber. As a result, the adaptive module centers the part that is attached to the base part of the sub-assembly. This is because the pressure difference in the uneven annular gaps "*C*" and "*B*" is proportional to the displacement of the assembled parts relative to each other. In other words, the low-pressure area (in the larger gap "*C*" or "*B*") coincides with the direction of skewing of the axes of the parts to be assembled. Thus, the alternate actuation of valves 22–25 according to the signals of the sensors of the pressure switch 18–21 leads to the supply of compressed air to one or another section I–IV of the corrugated chamber 6. As a result, chamber 6 is deformed and moves the gripper 10 in the direction of compensating for the relative misalignment of the assembled parts. In other words, the gripping device in which the attached part is located is automatically displaced in the direction of compensating for the positioning error of the robot arm.

4.2 Simulation an assembly module

If there is an error in the positioning of the robot arm at the beginning of the assembly of the shaft-sleeve connection parts, their primary contact can occur at one of the points "A" or "B" (Figure 4,a). For a more detailed study of the assembly process, we will choose a coordinate system Ox_0y_0, as shown in Figure 4(a). Then the coordinates of the characteristic points will be as follows: $C(\delta, y_c)$ the point is the midpoint of the segment *AB*; the point "*A*" of the contact of the parts to be assembled has coordinates $x_A = \delta - r\cos\alpha$; $y_A = y_c + r\sin\alpha$; coordinates of point "B" are: $x_B = \delta + r\cos\alpha$; $y_C = y_c - r\sin\alpha$ where: δ – is the positioning error of the robot arm; α – is the initial value of the skew angle of the axes of the assembled parts; $r = d/2$, d – is the inner diameter of the sleeve or the outer diameter of the shaft of the shaft-sleeve connection. Let us write down the equations of straight lines that coincide with the surfaces of the left and right chamfers of the shaft. A straight line runs along the left chamfer $y = ctg\gamma(x + r$, and a straight line runs along the right chamfer $y = -ctg\gamma(x - r)$, where: γ – is the angle between the vertical and the chamfer of the "shaft" type part (see Figure 4, a). Let us substitute in these equations the coordinates of the points "A" and "B" indicated above, respectively:

$$y_{CA} + r\sin\alpha = ctg\gamma(\delta - r\cos\alpha + r) \tag{1}$$

$$y_{CB} - r\sin\alpha = -ctg\gamma(\delta + r\cos\alpha - r) \tag{2}$$

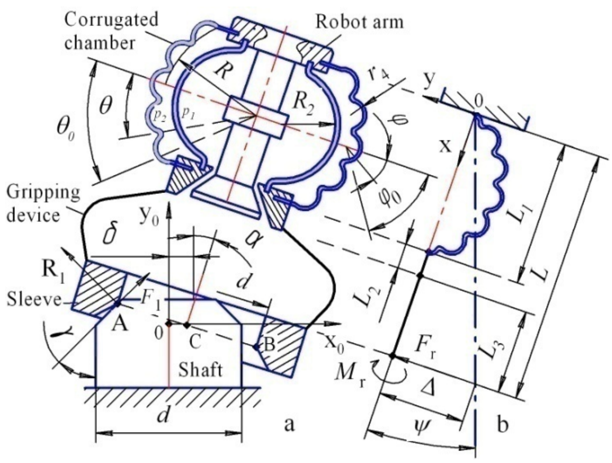

Figure 4. Diagram of the assembly process: a – a diagram of the interaction of the assembled parts of the "shaft-sleeve" type; b – diagram of the theoretical cantilever beam

From here we find the ordinate of point "C" when contact occurs at point "A" or point "B":

$$\begin{aligned} y_{CA} &= ctg\gamma(\delta - r\cos\alpha + r) - r\sin\alpha; \\ y_{CB} &= r\sin\alpha - ctg\gamma(\delta + r\cos\alpha - r) \end{aligned} \tag{3}$$

To determine at which point the contact of assembly objects occurs, we find the difference in the values of the ordinates (3):

$$y_{CA} - y_{CB} = 2(\delta ctg\gamma - r\sin\alpha) \tag{4}$$

If this difference has a positive value, then the contact of the collected parts occurs at point "A", and when the value (4) is negative, then the contact will be at point "B". And only when the difference (4) is equal to zero, the contact of the assembled parts will occur simultaneously at two points "A" and "B". For the process of assembling parts of the "shaft-sleeve" type to occur without jamming, the adaptive assembly module must contain elements of flexibility to compensate for the misalignment of parts of the "shaft-sleeve" type. In this case, such an element of compliance is a corrugated chamber (see Figure 2, item 6).

To simulate the behavior of the assembly module, we will interpret the module as a cantilever beam of variable stiffness. This assumption is quite acceptable from the point of view of the classical theory of strength of materials. The upper edge of this cantilever beam, which interprets the assembly module, is rigidly fixed to the robot arm, and the lower end of the theoretical cantilever beam is free. A force F_r (Figure 4,b) and a pair of forces with a moment M_r are applied to the lower end of the cantilever beam, which arises during the interaction of assembly objects of the "shaft-sleeve" type.

On the section of length L_1, the cross-section of the cantilever beam is a corrugated chamber, on the section of length L_2, the cross-section of this beam is a bushing with a tapered hole (see also Figure 2, item 7) and this bushing is attached to the corrugated chamber (Figure 2, pos. 6). The section of length L_3 is a gripping device that holds the bushing type to be connected. If contact occurs at point "*A*" [when the condition is satisfied $(\delta ctg\gamma - r\sin\alpha) > 0$, according to expression (4)], then a force and a pair of forces F_r with a moment M_r will act on the free end of the beam:

$$\begin{aligned} F_{\Gamma} &= R_1 \cos\gamma - kR_1 \sin\gamma; \\ M_{\Gamma} &= d(kR_1 \cos(\gamma-\alpha) + R_1 \sin(\gamma-\alpha))/2 \end{aligned} \tag{5}$$

where: R_1 – is the value of the normal reaction; k – coefficient of sliding friction, P – assembly force from the robot arm. Then the condition for the absence of jamming of assembly objects will look like this:

$$kR_1 \cos\gamma + R_1 \sin\gamma < P\,, \tag{6}$$

Under the action of these forces, the console beam bends and the gap "C" increases, and the gap "B" accordingly decreases, which leads to a redistribution of pressures and velocities of the outflow of compressed air from the oval chamber pos. 5 (see Figure 2). Then the corresponding pressure sensor is triggered (Figure 3) and the air is supplied to the corresponding compartment of the corrugated chamber, creating a pressure p_2 in it. Due to this pressure, an additional load will act on the beam, which is distributed along the section L_1 (Figure 4,b). The intensity of this load can be calculated by the formula

$$\begin{aligned} q(\theta) &= p_2 \int_{-\pi/4}^{\pi/4} R\cos^2\theta \cos\varphi_1 d\varphi_1 = \\ &= \sqrt{2} p_2 R \cos^2\theta \end{aligned} \tag{7}$$

where: R – is the inner radius of the corrugated chamber; θ – variable angle, which is determined by the beginning and end of the section L_1, i.e. the length of the corrugated chamber,

$$\theta_o = \arcsin(L_1/(2R)); \; -\theta_o \le \theta \le \theta_o \tag{8}.$$

Let us choose the origin of the coordinate system at the point of pinching of the console beam, as shown in (see Figure 4,b): we direct the *Ox* axis along the beam axis and the *Oy* axis perpendicular to the Ox axis. Then we can write expressions for the transverse forces *Q(x)* and bending moments *M(x)* on each section of the console beam, namely:

$$\begin{aligned} Q(x) &= F_r + \int_{\theta}^{\theta_o} q(\varphi_2)dz; \quad 0 \le x \le L_1; \\ M(x) &= M_r + F_r(L-x) + \int_{\theta}^{\theta_o} q(\varphi_2)(z-x)dz, \end{aligned} \tag{9}$$

where z – is the variable of the indicated integral. There are dependencies here: $x = R\sin\theta_o + R\sin\theta$;
$z = R\sin\theta_o + R\sin\varphi_2$; $dz = R\cos\varphi_2 d\varphi_2$;
$\theta \le \varphi_2 \le \theta_o$.

Substituting these dependences in (9) and performing the integration, we obtain formulas for the transverse forces *Q(x)* and bending moments *M(x)* in the section L_1, i.e. corrugated chamber length:

$$Q(x) = p_2 R^2 \sqrt{2}(\sin\theta_o - \sin\theta - \frac{1}{3}\sin^3\theta_o$$
$$+ \frac{1}{3}\sin^3\theta) + F_r;$$
$$M(x) = p_2 R^3 \sqrt{2}(\frac{\cos^4\theta - \cos^4\theta_o}{4} -$$
$$-\sin\theta(\sin\theta_o - \sin\theta -$$
$$-\frac{1}{3}\sin^3\theta_o + \frac{1}{3}\sin^3\theta)) + F_r(L-x) + M_r;$$
$$0 \le x \le L_1; \; -\theta_o \le \theta \le \theta_o$$

In other sections of the cantilever beam, namely in sections L_1 and L_2, the formulas for determining the shear forces *Q(x)* and bending moments *M(x)* are as follows:

$Q(x) = F_r$; $M(x) = M_r + F_r(L-x)$; $L_1 \le x \le L$ where $L=L_1+L_2+L_3$ (see Figure 4,б).

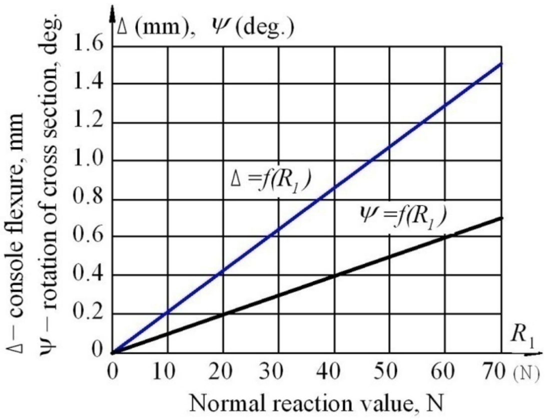

Figure 5. Dependence of the bend Δ of the end of the console and the angle of rotation *ψ* its cross-section on the value of the reaction R_1

The misalignment of the assembly objects is compensated for by displacement Δ (deflection of the cantilever beam) and the angle of rotation ψ of the cross-section of the free end of the specified beam. To determine these parameters, we apply at the end of the beam, respectively, a unit dimensionless force $N = 1$ or a unit dimensionless pair force $M_2 = 1$ and use the well-known Mohr integral:

$$\begin{aligned}\Delta &= \int_0^{L_1} \frac{(L-x)M(x)dx}{E_1 I_1} + \int_{L_1}^{L_1+L_2} \frac{(L-x)M(x)dx}{E_2 I_2} + \\ &+ \int_{L_1+L_2}^{L} \frac{(L-x)M(x)dx}{E_3 I_3} + k_1 \int_0^{L_1} \frac{Q(x)dx}{G_1 S_1} + \\ &+ k_2 \int_{L_1}^{L_1+L_2} \frac{Q(x)dx}{G_2 S_2} + k_3 \int_{L_1+L_2}^{L} \frac{Q(x)dx}{G_3 S_3}; \qquad (10) \\ \psi &= \int_0^{L_1} \frac{1 \cdot M(x)dx}{E_1 I_1} + \int_{L_1}^{L_1+L_2} \frac{1 \cdot M(x)dx}{E_2 I_2} + \\ &+ \int_{L_1+L_2}^{L} \frac{1 \cdot M(x)dx}{E_3 I_3}\end{aligned}$$

where: I_i – moments of inertia of the cross-sections of the beam parts; E_i – Young's moduli; G_i – shear moduli; Si is the cross-sectional area of the cantilever beam, respectively i – is the serial number, i.e. i = 1.2.3; k_i – coefficients that depend on the shape of the cross-section of the cantilever beam. For example, for a thin circular ring, $k_1 = 1$. Also, similarly to expressions (10), one can find the displacement of the end of the sections L_1 (the length of the corrugated chamber) to know how the dimensions of the gaps "*C*" and "*B*" change (see Figure 1 and Figure 2) through which the compressed air.

Based on the simulation results, graphical dependences of the bending of the end of the console Δ and the angle ψ of rotation of its cross-section on the value of the reaction force R_1 (Figure 5) at the points of contact of the assembly objects, as well as the dependence of these parameters on the value of pressure p_2 (Figure 6) in the corrugated chamber of the assembly module were obtained.

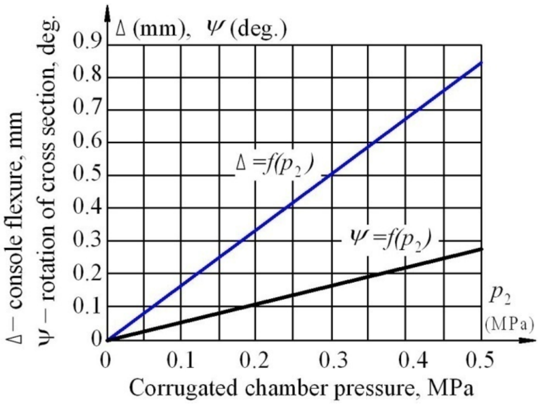

Figure 6. Dependence of the bend Δ of the end of the console and the angle of rotation ψ its cross-section from the value of pressure p_2

The modeling was carried out under the following initial conditions, which were determined from considerations of industrial feasibility, namely: polyvinyl chloride (PVC) was used as the material of the elastic chambers. This material is quite durable and has the following characteristics: specific density $1.35 \cdot 10^3$ … $1.43\psi \cdot 10^3$ (kg/m^3) ultimate strength: tensile $4 \cdot 10^7$ … $7 \cdot 10^7$ (Pa) and bending $8 \cdot 10^7$ … $12 \cdot 10^7$ (Pa); Young's modulus $2.6 \cdot 10^9$ … $4.0 \cdot 10^9$ (Pa) (Pa); the wall thickness of the corrugated polyvinyl chloride chambers was s = 2 mm. The ranges of errors in the mutual orientation of parts were: linear error δ = 0.1...1 (mm); angular error α = 0.1...2 (degree). The assembly force varied in the range P = 10...100 (N); the sliding friction coefficient of steel parts was k = 0.1... 0.3. Such characteristics of the assembly module are quite acceptable for industrial robots with a carrying capacity of 3 kg to 10 kg.

As can be seen from the graph in Figure 5, the achieved values of the bend of the corrugated chamber and the angles of rotation of its cross-section are quite sufficient to compensate for the error in the mutual orientation of the objects of the shaft-sleeve assembly. It should be noted here that the hand positioning error of modern industrial robots, as a rule, does not exceed 0.1...0.3 (mm). However, the error in the relative orientation of assembly objects increases significantly if the base component of the assembly is on a conveyor that has a significantly larger positioning error. Figure 6, which illustrates the dependence of the values of the bend of the corrugated chamber and the angles of rotation of its cross-section on the pressure in the corrugated chamber, shows the pressure control range up to 0.5 MPa. This pressure generation range is quite acceptable for modern medium power pneumatic compressors. The obtained simulation results prove the rationality of using the proposed adaptive assembly module for medium-duty industrial robots in the instrument-making and machine-building industries.

For the reliable operation of the adaptive assembly module, formulas are required for the engineering calculation of the ultimate stresses that arise in the material of elastic chambers during their deformation to compensate for the orientation error of the assembly objects. The specified stresses must not exceed the ultimate strength of the chamber material.

4.3 Determination of stresses in elastic chambers

Due to the action of the pressures p_1 and p_2 (see Figure 2 and Figure 4), stresses arise in the sections of the elastic chambers, which are evenly distributed over the thickness of the walls of the chambers. In the inner chamber (see pos. 5, Figure 2), due to the symmetry of the structure, the stresses in the meridional and annular directions will be equal $\sigma_M = \sigma_k$. These stresses can be determined from the equation of equilibrium of stresses in an elementary element of the chamber, namely:

$$\frac{\sigma_м s}{R_2} + \frac{\sigma_k s}{R_2} = p_1, \qquad (11)$$

where: R_2 – is the radius of the elastic chamber; s – is the wall thickness of the chamber; p_1 is the pressure in the chamber. From here we find

$$\sigma_{м} = \sigma_{k} = \frac{R_3}{2s} p_1 . \qquad (12)$$

If we substitute the above characteristics of the chamber material (polyvinyl chloride) into formula (12), then it is easy to make sure that these stresses are much less than the strength limit of the chamber material. In the corrugated chamber (see pos. 6, Figure 2), the pressure p_2 also gives rise to stresses σ_{2m} in the meridian direction and stresses σ_{2k} in the annular direction of the section of the chamber. To determine the stresses σ_{2m}, we draw a horizontal section of the corrugated chamber and compose the equilibrium equation in projection onto the vertical:

$$\begin{aligned} &\sigma_{2m} s(R\cos\theta + r_4\cos\varphi)(\frac{\pi}{2}\cos\varphi + 2) - \\ &-p_2\frac{\pi}{4}(R\cos\theta + r_4\cos\varphi)^2 = 0 \end{aligned} \qquad (13)$$

where: s – chamber wall thickness; R is the radius of the corrugated chamber; r_4 – is the radius of the corrugation of the chamber (see Figure 4); p_2 – is the pressure in the corrugated chamber; φ – is the deformation angle of the elementary corrugation of the chamber; θ – the angle of deformation of the section of the chamber. From expression (13) we find the voltage value in the meridional direction of the chamber cross-section:

$$\sigma_{2m} = p_2 \frac{\pi(R\cos\theta + r_4\cos\varphi)}{2s(\pi\cos\varphi + 4)} . \qquad (14)$$

Figure 7 shows the results of modeling the dependence of stresses in a corrugated chamber on pressure at different thicknesses “s” (mm) of the chamber walls and critical deformation of the corrugations at φ = 80 degrees. As can be seen from these graphs, even with the minimum wall thickness of the corrugated chamber made of polyvinyl chloride, the maximum stress is almost an order of magnitude less than the permissible value during stretching tensile $4{\cdot}10^7$ … $7{\cdot}10^7$ (Pa). This proves the reliability of the assembly module operation during critical deformation of the corrugated chamber to compensate for errors in the relative orientation of the assembly objects.

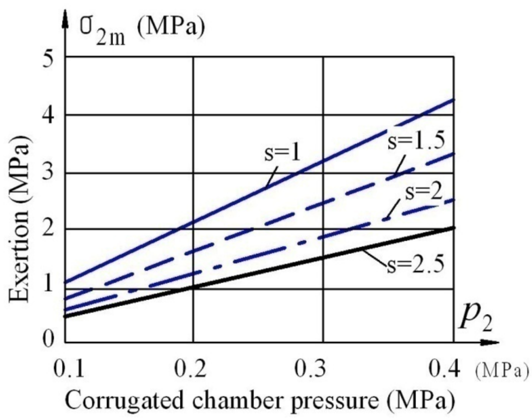

Figure 7. Dependences of stresses σ_{2m} in a corrugated chamber on pressure p_2 at different thickness s (mm) of the chamber walls

To determine the hoop stresses σ_{2k} in the section of the chamber, we conventionally cut out a small element from the chamber. Let us apply pressure p_2 to this element and compose the equilibrium equation for the selected element in projection onto the external normal. As a result, we get:

$$p_2 - \frac{\sigma_{2m} s}{r_4} - \frac{\sigma_{2k} s}{R\cos\theta + r_4\cos\varphi} = 0 . \qquad (15)$$

From expression (15), taking into account (14), we obtain the formula for hoop stresses

$$\sigma_{2k} = \frac{R\cos\theta + r_4\cos\varphi}{s}(p_2 - \frac{\sigma_{2m} s}{r_4}).$$

After transforming this expression, we obtain the formula for calculating the hoop stresses in the section of the corrugated chamber:

$$\begin{aligned} &\sigma_{2k} = \frac{R\cos\theta + r_4\cos\varphi}{s} p_2 \times \\ &\times\left(1 - \frac{\pi(R\cos\theta + r_4\cos\varphi)}{2r_4(\pi\cos\varphi + 4)}\right) \end{aligned} \qquad (16)$$

These stresses in the material of the chamber are much less than the stresses in the meridional direction, which are determined by the formula (14). Let us find the equivalent stress according to the classical fourth theory of strength of materials:

$$\sigma_e = \sqrt{\sigma_{2m}^2 + \sigma_{2k}^2 - \sigma_{2m}\sigma_{2k}} . \qquad (17)$$

Substituting the above values of the technical characteristics of the elastic chambers of the assembly module, it is easy to make sure that the equivalent stresses will be significantly less than the ultimate stress for the material of the corrugated chamber in the form of polyvinyl chloride. This excludes the destruction of the elastic chambers when compensating for the error in the relative orientation of the assembly objects and proves the reliability of the operation of the proposed adaptive assembly module for industrial robots.

5. RESULTS AND DISCUSSION

In contrast to the technical solutions discussed above in Section 2, the proposed assembly module makes it possible to compensate for errors in the relative orientation of assembly objects in the adaptation mode using simple and inexpensive industrial robots. The direction of compensation of the manipulator positioning error is determined by the pressure difference in the sections of the corrugated chamber, which connects the gripper to the robot arm. The actual adaptation mode to the assembly conditions is provided by automatic control of pressure differences using pressure sensors and the response of pneumatic valves, which direct compressed air to various sections of the corrugated chamber. The cost of the specified pneumatic automatics is much less than expensive servos and stepper motors.

As can be seen from the graphs in Figure 5 even at low contact forces (R = 20N…40N) of the assembly objects, the values of the linear and angular deformation of the corrugated chamber of the module are sufficient to compensate for the orientation error of the assembly objects.

Modern industrial robots have a positioning error in the range of 0.1...0.2 (mm), which is almost two times less than the indicated deformations of the elastic chamber. In this case, the required deformations of the corrugated chamber are achieved at a low compressed air pressure in the elastic chamber (see Figure 6). Therefore, to save the consumption of compressed air, pneumatic compressors of low power with a pressure of up to 0.3 MPa can be used.

The simulation results (see Figure 7) of the assembly module show that the stresses in the material of the elastic chambers (even with the minimum chamber wall thickness s = 1 mm and the maximum pressure p_2 = 0.4 MPa) are at least an order of magnitude less than the permissible material stresses in the form polyvinyl chloride. This circumstance guarantees reliable operation of the adaptive assembly module.

6. CONCLUSION

In this article, the authors propose an adaptive assembly device that is installed on the arm of an industrial robot of low cost and with a relatively low positioning accuracy. The device allows you to compensate for errors in the relative orientation of assembly objects in the mode of adaptation to the conditions of the assembly process. Positioning error compensation is determined by the pressure difference in the sections of the corrugated chamber of the assembly module. This effectively eliminates the need for expensive software to control the robot motors for each degree of freedom of movement of the robot arm.

The presence of elastic corrugated chambers, which are under low pressure of compressed air, makes it possible to automate the assembly of fragile parts or parts with a thin protective coating without additional dynamic loads. This is because the forces at the contact points of the assembly objects, which arise during deformation of the elastic pneumatic chambers, are several times less than the permissible forces for fragile parts or their thin protective coatings of chemical or galvanic origin. The obtained analytical dependencies provide an opportunity for engineers to carry out calculations of the parameters of an assembly module when designing it to equip inexpensive industrial robots.

Ultimately, the proposed adaptive assembly module makes it possible to use simple and inexpensive industrial robots to automate assembly processes, which in turn, by reducing financial capital investments, increases the economic efficiency of robotic assembly processes in serial and mass production.

DECLARATION OF CONFLICTING INTERESTS

The author(s) declared no potential conflicts of interest concerning the research, authorship, and/or publication of this article.

REFERENCES

[1] Chen H., Xu J., Zhang B. and Fuhlbrigge T. (2017). Improved parameter optimization method for complex assembly process in robotic manufac–turing. Industrial Robot, Vol. 44 No. 1, pp. 21-27. https://doi.org/10.1108/IR-03-2016-0098

[2] M. Penčić, M. Čavić, B. Borovac: Development of the Low Backlash Planetary Gearbox for Humanoid Robots. FME Transactions. Volume 45, 1, 2017. pp. 122–123.

[3] A. Deepak, R. Srivatsan, V. Samsingh. A Case Study on Implementation of Walking Worker Assembly Line to Improve Productivity and Utilisation of Resources in a Heavy Duty Manufacturing Industry. FME Transactions. Volume 45, 2017, 496-502.

[4] Pikalov A.A. (2014). Application of robotic systems in the assembly of aircraft structures. Branch of Irkut Corporation, Ulyanovsk, p. 1550–1555.

[5] Chen H., Zhang G., Zhang, H., Fuhlbrigge, T.A. Integrated robotic system for high precision assembly in a semi-structured environment, Assembly Automation. 27 (3), 247–252 (2007). DOI: 10.1108/014 45150710763277

[6] Wang, L., Sun, C., Tan, J., Zhao, B., and Wan, G. (2015). Improvement of location and orientation tolerances propagation control in cylindrical components assembly using stack-build assembly technique, Assembly Automation, Vol. 35 No. 4, pp. 358-366. https://doi.org/10.1108/AA-03-2015-023

[7] Jacobi P. Fiigemechanismenffir die automatisierte montage mil industrierobotern / P. Jacobi. TH Karl Marx Stadt, 1982, 96 p.

[8] Pitchandi, N., Subramanian, S.P. and Irulappan, M. (2017). Insertion force analysis of compliantly supported peg-in-hole assembly, Assembly Automation, Vol. 37 No. 3, pp. 285-295 https://doi.org/10.1108/AA-12-2016-167

[9] Jeong, K.W. and Cho H.S. (2009). Development of a pneumatic vibratory wrist for robotic assembly, Robotica. Cambridge University Press, 7(1), pp. 9–16. doi: 10.1017/S0263574700004987.

[10] Kolchugin E.I. (2011). Improving the efficiency of robotic assembly of cylindrical joints the use of passive adaptation and low-frequency vibrations. Dissertation of the candidate of technical sciences. Moscow: Moscow State Technical University, 2011, p. 159.

[11] Bozhkova L.V., Vartanov M.V., Kolchugin E.I. (2009). Experimental setup for robotic assembly on the basis of passive adaptation and low-frequency oscillations. Assembling in mechanical engineering, instrument making. 2009, No. 1, pp. 5–7.

[12] Vartanov, M.V., Bojkova, L.V. and Zinina, I.N. (2017). Mathematical model of robotic assembly by means of adaptation and low-frequency vibration, *Assembly Automation*, Vol. 37

No. 1, pp. 130-134. https://doi.org/10.1108/AA-04-2016-036

[13] Vartanov M.V. and Chan Chung Ta. (2020). Mathematical model of a robotic assembly in the presence of gripper rotation and low-frequency vibrations. Assembly in mechanical engineering, instrument making, No. 07, 2020, https://doi.org/10.36652/ 0202-3350-2020-21-7-299-304

[14] M. Polishchuk, M. Tkach. Experimental Studies of Robotic Assembly of Precision Parts. FME Transactions, ISSN / eISSN: 1451-2092. VOL. 49, No 1, 2021, pp. 44–55. https://www.mas.bg.ac.rs /istrazivanje/fme/start

[15] Ankit Sharma, Mathew Mithra Noel (2012). Design of a low-cost five-finger anthropomorphic robotic arm with nine degrees of freedom, Robotics and Computer-Integrated Manufacturing, Volume 28, Issue 4, 2012, pp. 551-558, ISSN 0736-5845, https://doi.org/10.1016/j.rcim.2012.01.001

[16] Jian Xu et al. (2021). Design and Characterization of a Spring Integrated Soft Hybrid Gripper. Design Engi–neering, 2021(02), 799-810.

[17] Srđan Savić, Mirko Raković, Marko Penčić, Milutin Nikolić et al. Design of an Underactuated Adaptive Robotic Hand with Force Sensing. Con–ference: 3rd International Conference on Electrical, Electronic and Computing Engineering – IcETRAN 2016, Zlatibor, Serbia, 13-16 June 2016, pp. ROI1.4-1–ROI1.4-5.

[18] Mikhail Polishchuk (2019). Anthropomorphic gripping device for an industrial robot: design and calculation of parameters, Springer Nature Applied Sciences (2019) 1:503. https://doi.org/10.1007 /s42452 -019-0535-z

[19] Min Li, Yueyan Zhuo, Jiazhou Chen, Bo He, Guanghua Xu, Jun Xie, Xingang Zhao & Wei Yao (2020). Design and performance character–rization of a soft robot hand with fingertip haptic feedback for teleoperation, Advanced Robotics 34:23, 1491–1505, doi: 10.1080/0169864.2020.182 2913.

АДАПТИВНИ МОНТАЖНИ МОДУЛ ЗА ИНДУСТРИЈСКЕ РОБОТЕ: ДИЗАЈН И СИМУЛАЦИЈА

М. Полишчук, С. Теленик, М. Ткач

У савременој производњи, аутоматизација процеса монтаже се постиже коришћењем индустријских робота високе прецизности позиционирања, као и елементима тактилне адаптације и скупог софтвера. У овом раду се предлаже алтернативни приступ решавању проблема смањења трошкова монтажних процеса. Овај приступ се састоји од употребе производног алата у облику меког адаптивног монтажног модула који је монтиран на руку робота. Предложени монтажни модул омогућава не само компензацију грешака у релативној оријентацији монтажних објеката, већ и искључује могућност оштећења ломљивих компоненти склопа или монтажних објеката са танким заштитним премазом хемијске или галванске природе. Овај ефекат се постиже употребом еластичних валовитих комора у структури модула, које, када се у њих доведе компримовани ваздух, исправљају положај једног од монтажних објеката.

Чланак нуди опис новог дизајна монтажног модула, као и нуди аналитичке зависности за прорачун пројектних параметара модула. Приказани су резултати моделирања параметара монтажног модула. Главни економски ефекат је смањење трошкова технолошке опреме за индустријске роботе уз задржавање способности прилагођавања условима процеса монтаже.